Institute of Physics Publishing Measurement Science and Technology

Meas. Sci. Technol. **17** (2006) 2852–2860 doi:10.1088/0957-0233/17/10/041

# Prototype cantilevers for SI-traceable nanonewton force calibration

**Richard S Gates and Jon R Pratt**

National Institute of Standards and Technology, Gaithersburg, MD 20899, USA

Received 3 May 2006, in final form 23 August 2006
Published 20 September 2006
Online at stacks.iop.org/MST/17/2852

**Abstract**
A series of extremely uniform prototype reference cantilevers has been created that can be used to calibrate the spring constants of atomic force microscopy (AFM) cantilevers and other micromechanical structures. By utilizing optimal combinations of material, design and the latest microfabrication processing techniques, arrays of cantilevers were created from single crystal (1 0 0) silicon. Nominal spring constants were estimated to be in the range 0.02 N m$^{-1}$ to 0.2 N m$^{-1}$. Resonance frequency measurements were used to assess the uniformity of devices from different portions of a silicon-on-insulator wafer and in different processing batches. Variations of less than 1% (relative standard deviation) in resonance frequency attested to the high degree of uniformity achieved. Independent calibration of cantilevers in an array using an electrostatic force balance indicated that the actual spring constants ranged from 0.0260 N m$^{-1}$ ± 0.0005 N m$^{-1}$ (±1.9%) to 0.2099 N m$^{-1}$ ± 0.0009 N m$^{-1}$ (±0.43%). The results confirm the feasibility of creating uniform reference cantilevers and calibrating them using a Système International d'Unités (SI)-traceable technique, making these devices excellent candidates as force calibration standards for AFM.

(Some figures in this article are in colour only in the electronic version)

## 1. Introduction

Atomic force microscopy (AFM) has become a very popular technique for imaging and probing the properties of surfaces down through the nanometer scale. The estimation of forces applied to surfaces during AFM experiments is not only important in nanomechanical property measurements, but also in imaging, where excessive forces can potentially cause distortions and movements in soft materials that alter the true topography, leading to improper interpretation of results. Accurate estimation of the forces applied to samples requires calibration of the spring constants of AFM cantilever probes. Until recently, however, there was no Système International d'Unités (SI) traceable AFM force standard below 5 $\mu$N [1, 2]. There are many different techniques for estimating the spring constants of cantilevers including solid mechanics or finite element modelling, resonance frequency [3, 4], energy balance [5–7] and reference force methods [8–10]. Some of these techniques are restricted to certain types of cantilevers (e.g. rectangular cantilevers, no metal coatings, etc) and the repeatability is normally no better than 10% to 20%[1] [7]. The absolute accuracy is unknown as none of these techniques are SI-traceable.

One of the most useful techniques for calibrating AFM cantilevers involves the use of a reference cantilever as a reference force. This technique, pioneered by Torii *et al* [8], Gibson *et al* [9] and Tortonese and Kirk [10], involves generating AFM force curves by probing the end of a 'known' cantilever. If the spring constant of the unknown cantilever is reasonably close (within a factor of 10) to the spring constant of the 'known' cantilever, the unknown spring constant can be estimated with a repeatability of about 10% as estimated in [7]. One significant advantage of this technique is that it applies to a wide variety of cantilever types including rectangular, triangular, metal-coated and even colloid probe.

[1] Unless otherwise specified, uncertainties expressed in this paper are ±1 standard deviation and relative uncertainties are ±1 standard deviation/mean and given in %.

Currently, there are commercial tipless reference cantilevers produced[2,3] with nominal spring constants estimated by the plan dimensions and measurement of a resonant frequency. The absolute accuracy is not verified, and uncertainties in the dimensional and material property estimates may lead to relative errors of 50% or more in the assigned spring constant values. A second source of reference cantilevers[4] consists of a set of regular commercial cantilever probes (with tips) that have been pre-calibrated using the added mass method [4] which typically has a repeatability of 10% to 20%. None of the commercially available reference cantilevers are SI-traceable.

Other researchers are attempting to create accurate calibration artefacts that could be used to calibrate AFM cantilevers. Cumpson *et al* [11] at the National Physical Laboratory (NPL) in the UK have produced a prototype reference cantilever that provides stiffness calibration references in the range of 25 N m$^{-1}$ through 0.03 N m$^{-1}$. The device consists of a large (150 $\mu$m wide, 1600 $\mu$m long) cantilever with fiducial marks that could allow precise alignment of the contact point for a cantilever-on-cantilever calibration. Measurements performed in our laboratory using the electrostatic force balance (EFB) and a calibrated instrumented indentation machine have yielded SI-traceable values for the stiffness of this artefact at three of its fiducial locations [12]. We note here that for the sample device received, there was a discrepancy between our reported SI values and the values that were published by NPL (as much as 30% at one point). Cumpson and Hedley [13] also introduced a microfabricated device they called an electrical nanobalance that was reported to cover a range of stiffness of 0.03 N m$^{-1}$ to 1 N m$^{-1}$ and was potentially traceable to the SI. Behrens *et al* [14] in the Physicalisch-Technische Bundesanstalt in Germany have created cantilever-type piezoresistive sensor prototypes with stiffnesses of 0.66 N m$^{-1}$ and 7.7 N m$^{-1}$ that could be used to calibrate AFM cantilevers. Calibration of the devices was performed using a 'compensation balance' which was a slightly modified commercially available mass comparator. None of these prototype cantilevers are currently available commercially.

This paper describes a study to produce a prototype reference cantilever array that could serve as a spring constant transfer artefact that would be traceable to the SI. The goal is to produce a standard reference material that could be sold by NIST that would serve as an SI-traceable reference for calibration of AFM cantilever spring constants.

## 2. Approach

The approach used in this study was to develop a microfabrication process capable of producing arrays of very uniform reference cantilevers and integrate these cantilevers into a larger effort to incorporate standardization and SI traceability. The design of the cantilevers incorporated features to reduce measurement uncertainties encountered during the cantilever calibration process. Participation in a Versailles Advanced Materials and Standards (VAMAS) technical working area (TWA29) effort to investigate methods of calibrating spring constants of cantilevers allowed refinement of the best procedures for obtaining repeatable values. Verifying the spring constants of the cantilevers using an EFB developed here at NIST [1] could provide the SI traceability. The key to this overall approach lies in production of sufficiently uniform distribution of cantilevers on a single Si wafer such that calibration of a smaller statistical subset of the cantilevers using the EFB would validate the entire wafer.

The following section considers the basic mechanics of cantilevers and the uncertainties that may be introduced through static and resonant measurements of stiffness. This is followed by a description of the design of the experimental cantilever array and its method of fabrication. Finally, results of property measurements on the experimental cantilevers are provided to attest to the uniformity and degree of microfabrication control achieved in this study.

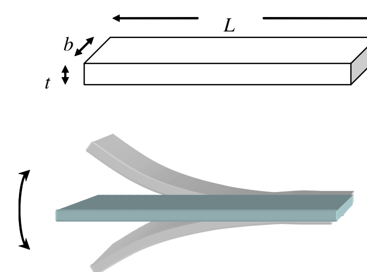


**Figure 1.** Idealized cantilever beam geometry used to estimate spring constant and first-mode resonance frequency.

## 3. AFM cantilever background

A commercial reference cantilever chip is available[5] that contains three reference cantilevers microfabricated from single crystal (1 0 0) Si. The cantilevers are rectangular, nominally 30 $\mu$m in width and 100 $\mu$m, 200 $\mu$m and 400 $\mu$m in length. This results in three spring constants that differ from each other by a factor of 8. The spring constants estimated by the manufacturer depend on the thickness of the actual cantilevers supplied, but are nominally on the order of 0.1 N m$^{-1}$, 1 N m$^{-1}$ and 10 N m$^{-1}$. As these reference cantilevers are close to a simple rectangular geometry (figure 1), they can be modelled as a simple Euler–Bernoulli beam [15] in order to estimate the spring constant, $k$:

$$k = \frac{E^* b t^3}{4L^3}, \qquad (1)$$

where $b$, $t$ and $L$ refer to width, thickness and length respectively and $E^*$ is the appropriate longitudinal elastic modulus. Width and length can be measured with reasonable accuracy. The major unknown in equation (1) is the thickness of the cantilever, which in the case of commercial reference cantilevers is on the order of 2 $\mu$m to 4 $\mu$m. Knowing this thickness value to 1% uncertainty would result in a 3% contribution to the spring constant uncertainty, and require

[2] CLFC, Veeco Probes, Santa Barbara, CA, USA.

[3] Certain commercial equipment, instruments or materials are identified in this paper to adequately specify the experimental procedure. Such identification does not imply recommendation or endorsement by the National Institute of Standards and Technology nor does it imply that the materials or equipment identified are necessarily the best available for the purpose.

[4] Asylum Research, Santa Barbara, CA, USA.

[5] CLFC, Veeco Probes, Santa Barbara, CA, USA.

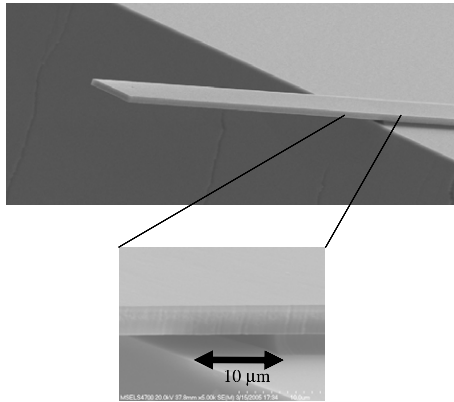


**Figure 2.** 10 $\mu$m overetch of commercial reference cantilever $SiO_2$ attachment layer observed by SEM.

a measurement accuracy of 20 nm. This is very difficult to achieve, especially when several measurements along the width and length of a cantilever would be required to check for thickness uniformity.

A second, dynamic, cantilever model can help to estimate the thickness from the first bending-mode resonance frequency. Assuming an ideal, monolithic, rectangular beam, fixed at one end (figure 1) and modelled as a simple harmonic oscillator, we can obtain, using the dynamic Euler–Bernoulli beam theory [16]

$$f_{\text{vac}} = 0.1615\frac{t}{L^2}\sqrt{\frac{E^*}{\rho}}, \tag{2}$$

where $f_{\text{vac}}$ is the first bending-mode resonance frequency in vacuum, and $\rho$ is the cantilever material density. In the case of single crystal Si, this is 2329 kg m$^{-3}$ (known to better than one part in $10^6$) [17]. Thus, the measured resonance frequency of a uniform rectangular reference cantilever can be used to estimate the thickness.

The accuracy of the above equation assumes of course that the correct values of $E^*$ and $L$ are used—not a trivial assumption. For example, SEM analysis of commercial reference cantilevers revealed an occasional over-etching of the oxide layer that joins the reference cantilever to the handle chip (figure 2). This particular feature resulted in a cantilever that is effectively 10 $\mu$m longer than that measured by the 'plan' dimensions usually evaluated. As a result, this error reduced the actual spring constant for the cantilever by 30% (for the shortest cantilever). More significant is the error that would be produced in the estimated spring constant by resonance frequency measurement. Increasing the length of the cantilever by 10% (shortest cantilever case) decreased the measured resonance frequency by 20%. Using this reduced resonance frequency and the original (plan) length dimension would propagate the error through to the thickness estimate, reducing it by 20%. The resulting spring constant estimate would be reduced by 60%. The net effect of the over-etching is that while the actual spring constant may decrease by 30%, the estimated $k$ decreases by 60%, a 30% undervaluation of the spring constant.

Errors may also be introduced through the use of an incorrect modulus. For an isotropic, *slender* beam ($b \ll t$), $E^* = E$, the plane stress or Young's modulus of the material. For a *wide* beam ($b \gg t$), most of the beam is under plane-strain constraint and $E^* = E/(1-\nu^2)$, the plane-strain modulus, where $\nu$ is Poisson's ratio of the material [15]. The problem is further compounded in that single crystal Si is elastically anisotropic and hence Young's modulus and Poisson's ratio in the correct direction must be used. For an ideal, *wide* beam (where $t \ll b \ll L$) microfabricated from a Si (1 0 0) wafer with the long axis of the cantilever aligned in the Si$\langle 1\,1\,0\rangle$ direction, the plane-strain elastic modulus is defined by

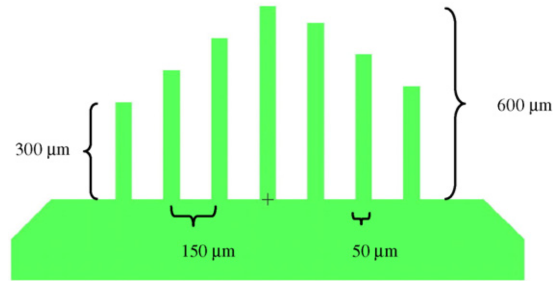


**Figure 3.** Experimental prototype reference cantilever array plan view (SOI device level).

$$E^* = \frac{E_x}{1-\upsilon_{xy}\upsilon_{yx}} = \frac{(C_{11}+2\cdot C_{12})\cdot(C_{11}-C_{12})}{2\cdot C_{11}} + C_{44}. \tag{3}$$

Using Si $C_{ij}$ values from McSkimin *et al* [18] the plane-strain elastic modulus is calculated to be $E^* = 169.8$ GPa. Note that Young's modulus and Poisson's ratio for Si vary as a function of orientation within the ranges of 130 GPa $\leqslant E \leqslant$ 187 GPa and $0.064 \leqslant \nu \leqslant 0.279$ [19], respectively; so considerable errors are possible if the incorrect modulus is used.

## 4. Experimental cantilever design

The prototype experimental cantilevers were designed to reduce microfabrication and measurement uncertainties. Single crystal silicon was selected because it has excellent material property uniformity ($E^*$, $\rho$). The basic design (figure 3) consisted of an array of seven rectangular, uniform cantilevers of varying length. This design is amenable to simple modelling as a check on process control and uniformity. From equation (1), it is obvious that the most critical dimensional parameters are thickness and length. Thickness was defined using high quality silicon-on-insulator (SOI) wafers with controlled device thickness uniformity. Length control was established using calibrated e-beam lithography to both accurately pattern the cantilevers onto the SOI and achieve the proper alignment of the cantilever pattern with the edge of the handle wafer chip.

Several design improvements over current commercial reference cantilevers were also made to optimize the ability to perform calibration measurements using the experimental cantilevers. The cantilever width was increased to 50 $\mu$m to make calibration measurements less susceptible to the effects of axial misalignment issues. The length was varied from 300 $\mu$m to 600 $\mu$m in increments of 50 $\mu$m. As no cantilever was less than 300 $\mu$m, these long reference cantilevers should be less susceptible to longitudinal misalignment during the

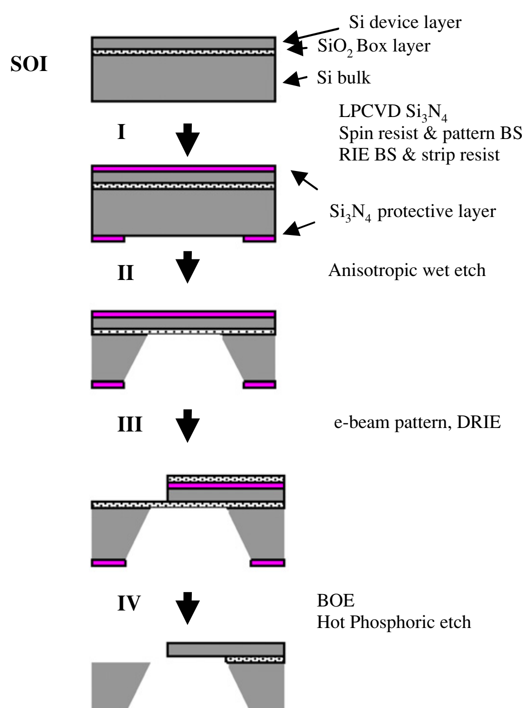


**Figure 4.** Microfabrication process flow summary.

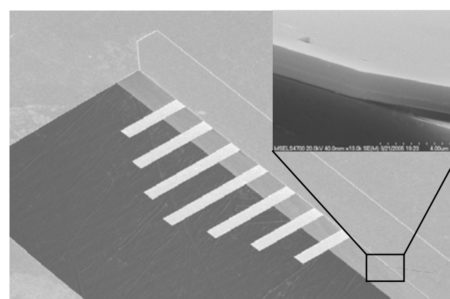

**Figure 5.** SEM photomicrograph of the experimental cantilever array with the inset showing device layer pattern overlay accuracy and no over-etch gap.

actual force curve calibration process. The design of an integral attachment ledge at the base of the cantilevers (shown in figure 3) in the SOI device level allowed pattern alignment overlay accuracy measurement using an SEM.

The combination of material properties and dimensions for the cantilevers in the experimental array produced cantilevers with nominal spring constants in the range of approximately 0.02 N $m^{-1}$ through 0.2 N $m^{-1}$.

## 5. Microfabrication

Silicon-on-insulator (SOI) wafers were used to maximize the cantilever thickness uniformity. According to the manufacturer's (Soitec—Grenoble, France) inspection report, the mean thickness of the Si device layer was 1.397 $\mu$m $\pm$ 0.017 $\mu$m ($\pm 6\sigma$ where $\sigma$ = standard deviation). Handle wafer thickness was nominally 350 $\mu$m.

The overall process flow is shown in figure 4 and consisted of a series of deposition, patterning and etching processes designed to accurately dimension the cantilevers while minimizing changes in the device layer thickness. In step I, an initial low pressure chemical vapour deposition (LPCVD) $Si_3N_4$ protective layer (130 nm thick) was applied to both sides of the wafer to protect the underlying Si during the anisotropic etching stages used to define the handle chip. Back side (BS) patterning of a resist was performed using contact optical lithography. Reactive ion etching (RIE) using $CF_4$ then removed the patterned $Si_3N_4$. In step II, anisotropic wet etching using KOH (25%, 90 °C) created the membrane for the cantilevers and defined the handle chip perimeter. For step III, e-beam lithography was used to locate the edge of the membrane and front side (FS) pattern the cantilever array in the proper position. FS patterning was performed on a hydrogen silsesquioxane (HSQ) negative e-beam resist. Deep reactive ion etch (DRIE) removed the non-patterned device layer. In step IV, buffered oxide etch (BOE) removed the buried and HSQ oxides and hot phosphoric acid removed the $Si_3N_4$ layer. The microfabrication process was designed to minimize alteration of the thickness of the device layer that would ultimately become the cantilever thickness. We estimate from etching selectivity parameters that only 10 nm of device silicon was removed during the microfabrication process, bringing the estimated final cantilever thickness to 1.387 $\mu$m.

Three process batches were made for this study using one-fourth sections of a single SOI wafer that were anisotropically etched (back side only) together in the same KOH bath. Each section front (cantilever) side was e-beam patterned, DRIE etched and released in separate processing batches.

## 6. Results

The cantilever arrays produced by microfabrication (figure 5) appeared to be very flat and uniform. Inspection of the plan dimensions in both SEM and using a white light interferometric microscope (WYKO NT8000, Veeco, Tucson, AZ, USA) confirmed the nominal dimensions and flatness of the cantilevers. SEM also confirmed the excellent patterning registration of the e-beam technique and the lack of any significant overetch of the $SiO_2$ attachment layer (inset of figure 5).

While the actual dimensions obtained from the microfabrication process are of interest, ultimately the most important parameter is the uniformity of the spring constants for the cantilevers from different parts of a wafer. This statistical uniformity will determine the potential accuracy of the traceable calibration of an entire wafer of devices. Since tests using the EFB require hours to days for each calibration, it is not feasible to use the EFB to measure the statistical uncertainty in the spring constants from array-to-array within the wafer. Inspection of the terms in equations (1) and (2) indicates that both spring constant ($k$) and resonance frequency ($f$) depend on the same two critical parameters of thickness and length, just to different degrees. Spring constant varies with the cube of both thickness and length (inverse), while $f$ varies with thickness to the first power and length (inverse) squared. This suggests that uniformity of the resonance frequency can serve as an indicator of the uniformity of $k$. In the worst case,

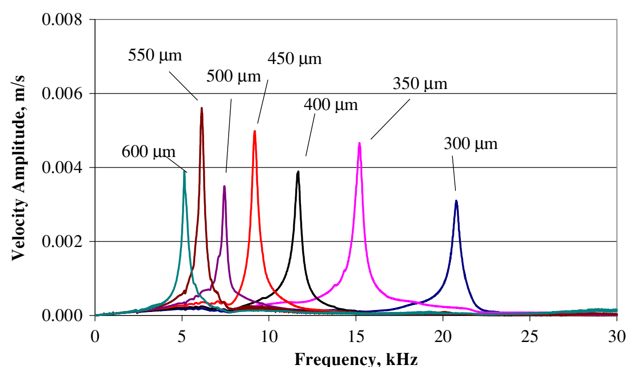


**Figure 6.** Resonant frequency spectra for experimental cantilevers in an array.

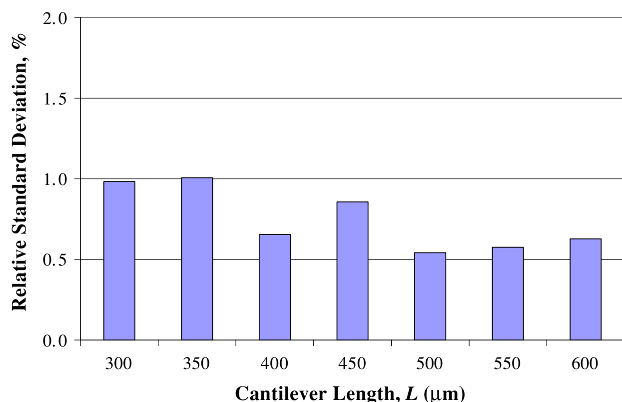


**Figure 7.** Resonance frequency uniformity from one wafer section.

if all of the variation comes from thickness, the effect on $k$ could be estimated by multiplying the resonance frequency uncertainty by a factor of 3.

Resonance frequencies were measured using a laser Doppler vibrometer (LDV) microscope (Polytec PI MSV 300, GmbH, Karlsruhe, Germany). A frequency range of 1 kHz to 50 kHz was used with a nominal resolution of 0.008 kHz. An example of the resonance peaks obtained on the experimental cantilever array using this instrument is shown in figure 6. A five-point smoothing was applied to the spectra prior to determination of the peak maxima.

A series of resonance frequency measurements made on each length of cantilever from a single wafer section (approximately 7 to 9 samples each) achieved very good uniformity as shown in figure 7. Relative standard uncertainty (1 std dev./mean) averaged 0.75%. When this measurement was expanded to a sampling of 15 to 22 cantilevers of each length, across three different processing batches, the relative uncertainty increased only slightly to 0.94%.

Similar resonance frequency measurements were made on a batch of five commercial cantilever sets (three cantilevers on each chip) from a single processing batch. The relative standard uncertainty was approximately 10%. The experimental cantilevers therefore represent an order of magnitude improvement in uniformity. Given this level of uncertainty in the chip-to-chip resonance frequency measurement, the uncertainty in $k$ is probably better than 3% (1 std dev.) and if the spring constants of these cantilevers

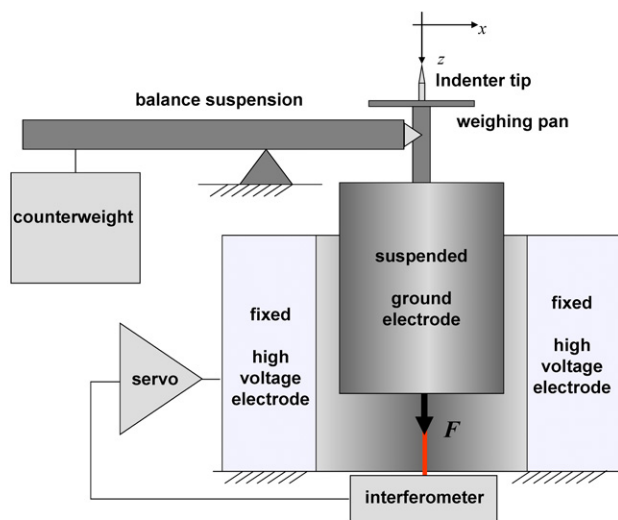


**Figure 8.** Schematic of the electrostatic force balance (EFB).

can be independently verified through the EFB, then an SI-traceable calibration can be realized with reasonable accuracy.

## 7. Electrostatic force balance calibration

The EFB was designed and constructed at NIST to realize an SI-traceable force measurement capability at the millinewton through nanonewton range (1). It is located in the NIST Advanced Measurement Laboratory (AML) in a nominal class 10 000 clean room, 12 m underground, in a temperature controlled (±0.01 °C) laboratory. The actual device itself is housed in a vacuum chamber to reduce disturbances from air currents. The EFB has been utilized for calibrating a piezoresistive cantilever with a spring constant near 1 N m$^{-1}$ [1].

The EFB consists of an electrostatic force generator that acts along a vertical axis ($z$-direction) aligned to the local gravity to within a few milliradians. The force generator comprises a pair of nested, coaxial cylinders as shown schematically in figure 8. The high-voltage cylinder is fixed while an inner electrically grounded cylinder is attached to a movable balance suspension, which can vary the degree of overlap between the cylinders. The capacitance, $C$, of this geometry is a linear function of the cylinders' overlap, and the gradient of capacitance, $\mathrm{d}C/\mathrm{d}z$, can be precisely measured by translating the inner cylinder with respect to the outer while using an interferometer and a high resolution capacitance bridge to map the capacitance as a function of the relative displacement. The voltage on the balance is servo controlled to maintain a fixed relative displacement between the cylinders by using an interferometer for displacement feedback.

The electrical force ($F$) generated by the cylinders for a given applied voltage is

$$F = \frac{1}{2}\frac{\mathrm{d}C}{\mathrm{d}z}\left(V_1^2 - V_2^2 + 2V_s(V_1 - V_2)\right), \qquad (4)$$

where $F$ is the force, $V_1$ is the control voltage applied to the outer electrode before a load is applied to the balance, $V_2$ is the voltage applied to the outer electrode after loading and $V_s$ is the potential difference between the electrodes resulting

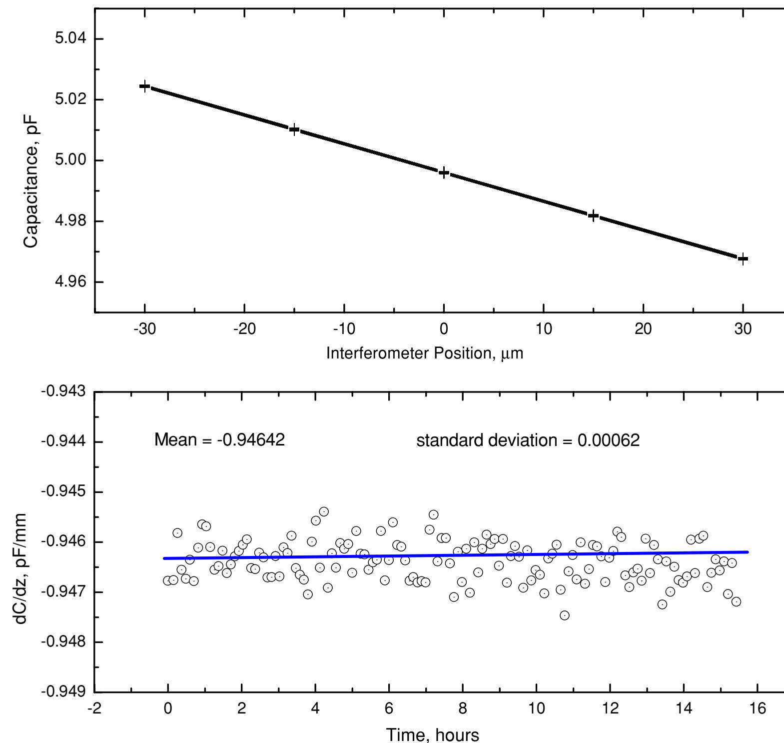


**Figure 9.** Capacitance as a function of interferometer position. The upper plot shows overlaid raw data obtained from 210 traverses of a 60 $\mu$m range of motion. The bottom plot records the slope that was fit to each of the traverse cycles along with the mean and standard deviation of the fits.

from surface potentials. The system has been used as a null balance to compare the computed electrical force to a known deadweight mechanical load of nominally 20 $\mu$N. An agreement between these two measurements is better than one part in $10^4$ [2].

We calibrated cantilever spring constants using a method proposed in [2], in which the EFB is used like an instrumented indentation machine to record force–displacement data, ensuring that both the force and displacement measurements are traceable, and measured along the same, well-defined line of action. A nominal 2 $\mu$m radius cono-spherical indenter tip (Hysitron Inc., Minneapolis, MN, USA) was mounted on the EFB weighing pan. The cantilever under test was manipulated using an automated fine motion stage and a microscope, both of which were in the vacuum chamber, to position the cantilever and bring it into contact with the indenter tip. Once contact was established, force–displacement data were gathered by an automated servo controller and data acquisition computer that automatically cycled the balance through a series of displacement setpoints. The electrostatic force required to deflect the cantilever while it was in contact with the balance was recorded along with the interferometer displacement reading. The force–displacement data were fitted using a least squares straight line, and the slope of this line was taken as the measured stiffness of the combined cantilever and balance, $k_m$.

As might be expected, $k_m$ must be corrected for the stiffness of the balance, which is the stiffness $k_b$ measured when no cantilever is present. Furthermore, it is necessary to determine the so-called load frame stiffness $k_l$, which is the stiffness measured when a rigid sample is introduced between the indenter tip and fixed support. The unknown cantilever stiffness, $k$, is then computed from the measured stiffness $k_m$ as

$$\frac{1}{k} = \frac{1}{k_m - k_b} - \frac{1}{k_l}. \tag{5}$$

Both ascending and descending forces were applied to take out any drift that was approximately linear with time.

### 7.1. EFB results

A typical capacitance gradient measurement is shown in figure 9, where capacitance is measured as a function of displacement from null position. Total displacement was $\pm 30$ $\mu$m. The measured gradient of $\mathrm{d}C/\mathrm{d}z = 0.9464$ pF mm$^{-1}$ agrees to within three parts in $10^4$ with the value recorded 6 months earlier of $\mathrm{d}C/\mathrm{d}z = 0.9467$, and our recent experience suggests that the gradient can be measured reliably with a relative uncertainty of two parts in $10^5$, provided care is taken to wait for temperature transients to settle out that are experienced during the pump down to vacuum.

Figure 10 shows the force–displacement data for the balance alone when it was cycled $\pm 5$ $\mu$m about an offset position. Five of the thirty recorded traverses are shown, and the drift is evident. Each individual cycle was fitted with a straight line and a slope determined. The mean value determined for the complete slope data set was $k_b = 0.034\,08$ N m$^{-1}$ $\pm$ 0.0004 N m$^{-1}$, where the uncertainty is 1 standard deviation of the sixteen values.

Load frame compliance proved more difficult to determine. The indenter was brought into contact with the cantilever handler chip, but the servo control system lacked sufficient bandwidth to remain stable for such a large change

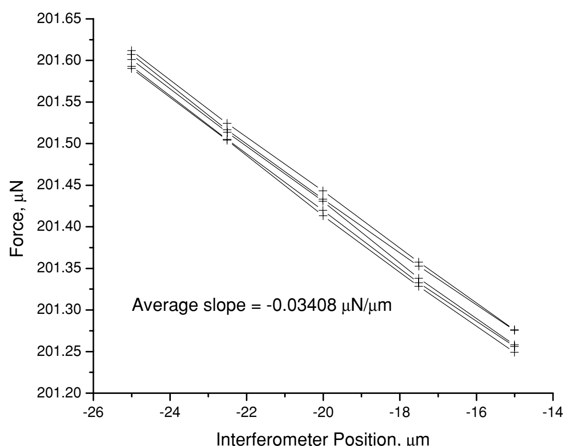


**Figure 10.** Force-displacement data for the balance alone (only 5 of 30 plots shown).

in effective balance stiffness. Servo control was disabled, the system was brought up to air and a value for load frame compliance estimated by manually applying approximately −10 mN deadweight preload to push the indenter tip into the chip surface (a 1 g mass was placed on the counterweight side of the balance). The electrostatic force was then cycled between 0 and 0.36 mN and the change in position recorded. The average deflection was 50 nm ± 10 nm. Combining these observations, we estimate $k_l = 7300\ \mathrm{N\ m^{-1}} \pm 1500\ \mathrm{N\ m^{-1}}$. For the cantilevers studied, the load frame stiffness ($k_l$) correction was negligible.

The shortest and longest experimental cantilevers in an array were selected for calibration using the EFB in order to check the feasibility of this approach. Measurements were taken by contacting the indenter tip with a location on the cantilever approximately 2 $\mu$m from the end of the cantilever (the tip appeared approximately one tip radius from the end of the cantilever when viewed through a microscope). Force–displacement data recorded during a test of the longest cantilever (600 $\mu$m) are shown in figure 11, as an example of a typical data set for the determination of cantilever stiffness. As in the case of the balance stiffness, there was a slow, long-term drift but this was on a time scale that did not significantly affect the slope values of each data set.

Measured spring constants were corrected for the total length of the cantilever using the cubic relationship between $k$ and $L$ (equation (1)). The shortest (300 mm) cantilever was measured at 0.2099 N m$^{-1}$ ± 0.0009 N m$^{-1}$ (0.43%). The longest cantilever (600 mm) was measured at 0.0260 N m$^{-1}$ ± 0.0005 N m$^{-1}$ (1.9%). The uncertainties were calculated using the summation of the variances of $k_m$ and $k_b$. The measured value for the smallest spring constant in the array approached the resolution limit of the EFB. The results are encouraging and demonstrate the feasibility of using the EFB to calibrate the cantilever arrays fabricated for this study.

A comparison of measured and calculated values of resonance frequency and spring constants for the actual cantilever array used in this study is provided in table 1 along with estimates of quality ($Q$) factors for the measured resonance peaks based on fitting the raw spectra to a simple harmonic oscillator model. The Euler–Bernoulli resonance

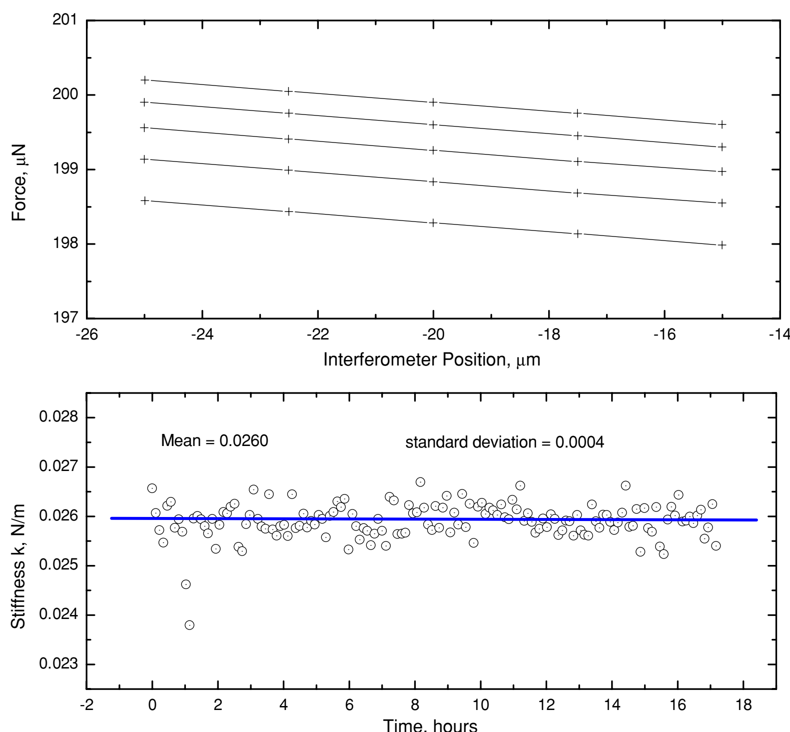


**Figure 11.** Force as a function of interferometer position for the 600 $\mu$m long experimental cantilever. The upper plot shows raw data obtained from 5 of the 298 traverses (every 60th traverse) of a 10 $\mu$m range of motion. The bottom plot records the corrected stiffness ($k$) derived from the slope that was fit to each of the 149 traverse cycles, along with the mean and standard deviation of the data.

**Table 1.** Comparison of measured and Euler–Bernoulli (EB) calculated values for experimental prototype cantilever array.

| | Resonance frequency, $f_o$ | | | | Spring constant, $k$ | | | |
|---|---|---|---|---|---|---|---|---|
| Cantilever length ($\mu$m) | $f_{meas}$ Air LDV (kHz) | $f_{EB}$[a] Air[b] (kHz) | $\Delta$ ($f_{meas} - f_{EB}$) (%) | $Q$[c] Air | $k_{EB}$[a] (N m$^{-1}$) | $k_{meas}$ EFB (N m$^{-1}$) | $k_{EBf}$[d] (N m$^{-1}$) | $\Delta$ ($k_{meas} - k_{EBf}$) (%) |
| 300 | 21.17 | 20.93 | 1.2 | 50 | 0.2098 | 0.2099 | 0.2147 | −2.2 |
| 350 | 15.50 | 15.35 | 1.0 | 42 | 0.1321 | | 0.1346 | |
| 400 | 11.81 | 11.74 | 0.6 | 37 | 0.0885 | | 0.0895 | |
| 450 | 9.30 | 9.26 | 0.4 | 31 | 0.0621 | | 0.0626 | |
| 500 | 7.48 | 7.50 | −0.1 | 28 | 0.0453 | | 0.0452 | |
| 550 | 6.22 | 6.19 | 0.5 | 24 | 0.0340 | | 0.0344 | |
| 600 | 5.20 | 5.19 | 0.2 | 20 | 0.0262 | 0.0260 | 0.0263 | −1.1 |

[a] Using $E^* = 169.8$ GPa, $t = 1.387$ $\mu$m, $b = 50.0$ $\mu$m, $\rho = 2329$ kg m$^{-3}$ and appropriate $L$ and Euler–Bernoulli equation (1) or (2).
[b] $f_o$ correction for air using the viscous method described in [20] using $\rho_{air} = 1.18$ kg m$^{-3}$ and $\eta_{air} = 1.84 \times 10^{-5}$ kg m$^{-1}$ s$^{-1}$.
[c] $Q$ estimated (±5%) using simple harmonic oscillator fit to resonance peak.
[d] Using equation (5) ($L$, $b$, $t$ dimensions and $\rho$ values above, and measured resonance frequency for actual cantilever array used, corrected for vacuum using the method[b] above).

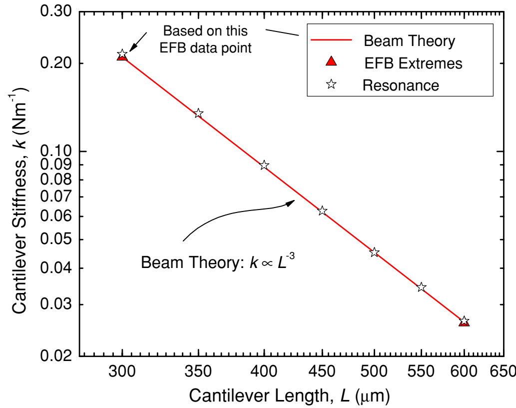


**Figure 12.** Spring constant measurements on an experimental cantilever array. Measurement uncertainties were smaller than the size of the symbols and were omitted for clarity.

frequencies were first estimated in vacuum using equation (2) with the constants listed and then corrected for air using the viscous method of Chon *et al* [20]. For the cantilevers in this study, this is only a 1.5% to 2.3% correction, depending on the length of the cantilever. The EB model values agree with the actual measured resonance frequencies to 1%. Spring constants for each cantilever were also calculated using the Euler–Bernoulli beam theory (equation (1)) from the nominal dimensions and measured resonance frequency. This is obtained by eliminating $E^*$ between equations (1) and (2) to yield

$$k = 9.582 Lbt\rho f_{vac}^2. \tag{6}$$

These model-calculated values agree with the EFB-measured values to 2%.

The EFB calibration data are also plotted in figure 12 to graphically demonstrate the agreement of the data with the Euler–Bernoulli beam theory. The two EFB data points are shown as solid triangles along with the $L^{-3}$ relationship for $k$ predicted by equation (1) (solid line) pinned only at the uppermost EFB-measured value. The lower EFB data point falls on the line indicating a good agreement with the theory. The hollow stars are calculated spring constants estimated using Euler–Bernoulli and measured resonance frequencies ($k_{EBf}$) as provided in table 1. The excellent agreement of the resonance frequency data with the beam theory extrapolation attests to the high degree of control achieved in the microfabrication process and supports the assumption that the experimental cantilevers can be accurately modelled as uniform, rectangular Euler–Bernoulli beams.

Initial calibration of a test cantilever using a reference cantilever from this work confirmed the ability to measure a spring constant with a repeatability of ±10%, as indicated by Burnham *et al* [7]. We are currently exploring the issues of spring constant matching, friction and probe tip alignment during the calibration procedure in order to optimize the calibration precision.

## 8. Conclusions

A prototype reference cantilever array has been designed and fabricated that can be used to calibrate AFM cantilevers using the reference cantilever method. Initial evaluation of cantilever arrays from three different microfabrication processing batches within a single wafer suggest that excellent cantilever uniformity can be achieved. Variations in resonant frequency of less than 1% (average relative standard deviation) were observed, which represent an order of magnitude improvement over commercially available reference cantilevers. This high degree of device uniformity offers the potential for qualifying an entire wafer of cantilevers using a smaller statistical subset for spring constant calibration using an independent method.

It has been demonstrated that an EFB is capable of calibrating these cantilevers in an SI-traceable way down to the smallest spring constant in the experimental array with an uncertainty of better than 2%. An agreement between the EFB-measured stiffness values and stiffness estimated using resonance frequency measurements and dimensional and material property values attest to the suitability of modelling the experimental cantilevers as uniform Euler–Bernoulli beams.

These results confirm the feasibility of the overall approach outlined in this paper and pave the way for production of SI-traceable force calibration reference artefacts that could

be made available to the AFM community. Work is continuing to address some of the more practical issues of microfabricated device yield and improved handle chip design, and also to refine the actual reference cantilever calibration procedures to obtain optimal results.

## Acknowledgments

The microfabrication was performed in part at the Cornell NanoScale Facility (CNF—Ithaca, NY), a member of the National Nanotechnology Infrastructure Network, which is supported by the National Science Foundation (Grant ECS 03-35765). RSG would like to thank John Treichler of the CNF for his excellent guidance throughout the critical e-beam lithography process. The authors would like to thank Dr Edwin R Fuller Jr of the Nanomechanical Properties Group, Ceramics Division, NIST for his calculation of the plane-strain elastic modulus for our cantilever beam orientation. We would also like to thank Dr Michael Gaitan of the MEMS Group, Semiconductor Electronics Division, NIST for the use of their laser Doppler vibrometer microscope for the resonance frequency measurements.

## References

[1] Pratt J R, Smith D T, Newell D B, Kramar J A and Whitenton E 2004 Progress toward Systeme International d'Unites traceable force metrology for nanomechanics *J. Mater. Res.* **19** 366–79

[2] Pratt J R, Kramar J A, Newell D B and Smith D T 2005 Review of SI traceable force metrology for instrumented indentation and atomic force microscopy *Meas. Sci. Technol.* **16** 2129–37

[3] Sader J E, Chon J W M and Mulvaney P 1999 Calibration of rectangular atomic force microscope cantilevers *Rev. Sci. Instrum.* **70** 3967–9

[4] Cleveland J P, Manne S, Bocek D and Hansma P K 1993 A nondestructive method for determining the spring constant of cantilevers for scanning force microscopy *Rev. Sci. Instrum.* **64** 403–5

[5] Hutter J L and Bechhoefer J 1993 Calibration of atomic-force microscope tips *Rev. Sci. Instrum.* **64** 1868–73

[6] Butt H J and Jaschke M 1995 Calculation of thermal noise in atomic-force microscopy *Nanotechnology* **6** 1–7

[7] Burnham N A, Chen X, Hodges C S, Matei G A, Thoreson E J, Roberts C J, Davies M C and Tendler S J B 2003 Comparison of calibration methods for atomic-force microscopy cantilevers *Nanotechnology* **14** 1–6

[8] Torii A, Sasaki M, Hane K and Okuma S 1996 A method for determining the spring constant of cantilevers for atomic force microscopy *Meas. Sci. Technol.* **7** 179–84

[9] Gibson C T, Watson G S and Myhra S 1996 Determination of the spring constants of probes for force microscopy/spectroscopy *Nanotechnology* **7** 259–62

[10] Tortonese M and Kirk M D 1997 *Characterization of application specific probes for SPM, Proc. SPIE* **3009** 53–60

[11] Cumpson P J, Clifford C A and Hedley J 2004 Quantitative analytical atomic force microscopy: a cantilever reference device for easy and accurate AFM spring-constant calibration *Meas. Sci. Technol.* **15** 1337–46

[12] Shaw G A, Kramar J and Pratt J 2007 SI-traceable spring constant calibration of microfabricated cantilevers for small force measurement *Exp. Mech.* at press

[13] Cumpson P J and Hedley J 2003 Accurate analytical measurements in the atomic force microscope: a microfabricated spring constant standard potentially traceable to the SI *Nanotechnology* **14** 1279–88

[14] Behrens I, Doering L and Peiner E 2003 Piezoresistive cantilever as portable micro force calibration standard *J. Micromech. Microeng.* **13** S171–7

[15] Timoshenko S P and Goodier J N 1983 *Theory of Elasticity* (New York: McGraw-Hill)

[16] Meirovitch L 1997 *Principles and Techniques of Vibrations* (Englewood Cliffs, NJ: Prentice-Hall)

[17] Deslattes R D, Henins A, Bowman H A, Schoonover R M, Carroll C L, Barnes I L, Machlan L A, Moore L J and Shields W R 1974 Determination of the Avogadro constant *Phys. Rev. Lett.* **33** 463–6

[18] McSkimin H J and Andreatch P Jr 1964 Measurement of third order moduli of silicon and germanium *J. Appl. Phys.* **33** 3312–9

[19] Brantley W A 1973 Calculated elastic constants for stress problems associated with semiconductor devices *J. Appl. Phys.* **44** 534–5

[20] Chon J W M, Mulvaney P and Sader J E 2000 Experimental validation of theoretical models for the frequency response of atomic force microscope cantilever beams immersed in fluids *J. Appl. Phys.* **87** 3978–88